PROCEEDINGS OF SPIE

SPIEDigitalLibrary.org/conference-proceedings-of-spie

Composites impact damage detection and characterization using ultrasound and x-ray NDE techniques

Shoukroun, Dana, Massimi, Lorenzo, Endrizzi, Marco, Bate, David, Olivo, Alesandro, et al.

Dana Shoukroun, Lorenzo Massimi, Marco Endrizzi, David Bate, Alesandro Olivo, Paul Fromme, "Composites impact damage detection and characterization using ultrasound and x-ray NDE techniques," Proc. SPIE 11381, Health Monitoring of Structural and Biological Systems XIV, 113810B (22 April 2020); doi: 10.1117/12.2549078

SPIE.

Event: SPIE Smart Structures + Nondestructive Evaluation, 2020, Online Only

Composite Impact Damage Detection and Characterization using Ultrasound and X-ray NDE Techniques

Dana Shoukroun[a, c], Lorenzo Massimi[a], Marco Endrizzi[a], David Bate[b], Alesandro Olivo[a], Paul Fromme[c]

[a] Department of Medical Physics and Bioengineering, University College London, UK
[b] Nikon, X-Tek Systems Ltd., Tring, UK
[c] Department of Mechanical Engineering, University College London, UK

ABSTRACT

Combining low weight and high strength, carbon fiber reinforced composites are widely used in the aerospace industry, including for primary aircraft structures. Barely visible impact damage can compromise the structural integrity and potentially lead to failures. Edge Illumination (EI) X-ray Phase Contrast imaging (XPCi) is a novel X-ray imaging technique that uses the phase effects induced by damage to create improved contrast. For a small cross-ply composite specimen with impact damage, damage detection was compared to ultrasonic immersion C-scans. Different defect types could be located and identified, verified from the conventional ultrasonic NDE measurement.

Keywords: CFRP, XPCi, Radiography, Ultrasonic

1. INTRODUCTION

Carbon fiber laminate composites provide good strength to weight ratio for aerospace applications. Manufacturing imperfections and impacts during the operation and servicing of the aircraft can lead to barely visible impact damage. Such impact can lead to defects such as delaminations, matrix or fiber cracking, fiber breakage and debonding, which reduce the load carrying capacity of the structure, and potentially compromise the structural integrity of the composite [1]. Nondestructive Evaluation (NDE) techniques allow for the localization and identification of damage induced in composite plates, with ultrasonic imaging and conventional, absorption-based radiography among the techniques most often used in industry. However, these techniques have several limitations; Ultrasonic imaging is often used for the localization of damage in composite plates, however its relatively low resolution prevents the identification and separation of multiple defects, as well as the detection of micro-defects [2]. Conventional radiography offers a much higher resolution, and thus a more accurate representation of damage within a given sample [3]. However, for carbon fiber-reinforced polymers, radiography encounters difficulties in resolving features due to the similar absorption coefficients of the components involved.

X-ray phase contrast imaging (XPCi) is a new imaging technique relying on the phase effects occurring due to the introduction of an object into the X-ray beam. Edge Illumination X-Ray Phase Contrast Imaging (EI XPCi) is a differential phase imaging technique, i.e., it detects phase changes from changes in the X-ray propagation direction (refraction angle), arising from distortions in the X-ray wave front [4, 5]. EI XPCi allows for the simultaneous acquisition and retrieval of the conventional absorption, refraction, and ultra-small angle scattering (USAXS, also referred to as dark field) images, with the latter being a representation of scattering signals in the micro-radian range caused by features in the sub-pixel scale [6]. EI XPCi is robust against X-ray energy variation and environmental vibrations, thus allowing it to be used in a laboratory environment. Other advantages of this method include the possibility of using divergent and polychromatic beams, and its insensitivity to increasing focal spot and pixel size, which can be problematic for other XPCi methods [4]. XPCi is highly sensitive to porosity and boundaries between materials, making it potentially a powerful tool for the detection of defects in composite materials. XPCi was previously used to investigate impact damage in composite structures.

Health Monitoring of Structural and Biological Systems XIV, edited by Paul Fromme, Zhongqing Su, Proc. of SPIE Vol. 11381, 113810B · © 2020 SPIE
CCC code: 0277-786X/20/$21 · doi: 10.1117/12.2549078

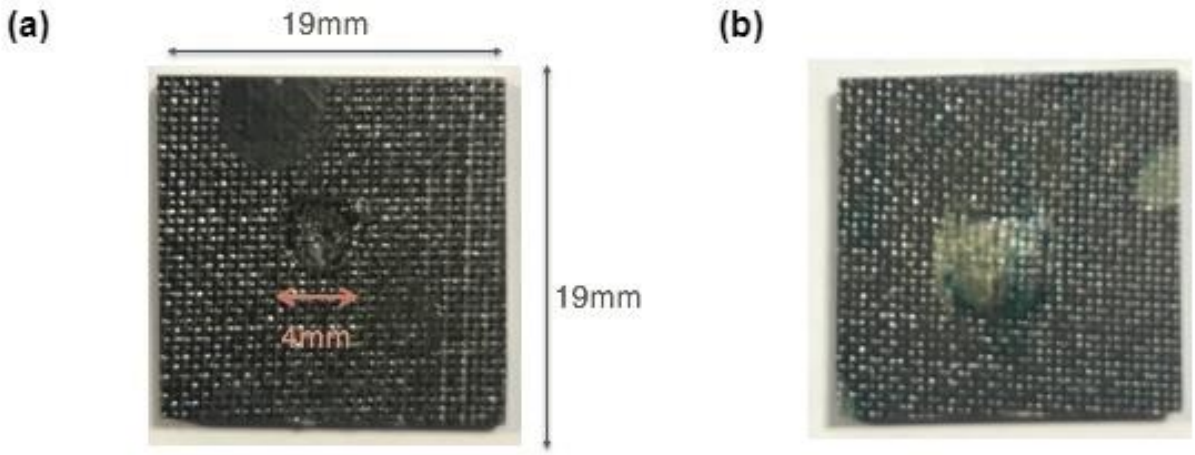

Fig. 1: Photograph of specimen (a) front surface showing indent and (b) showing back surface, with protrusion, resulting from direct impact.

Third generation synchrotron radiation was used to image a cracked silicon carbide (SiC) macro-fiber (140 μm diameter) in a composite plate, showing that phase contrast imaging was more sensitive to the variations in inhomogeneity than conventional X-ray imaging [7]. Free space propagation XPCi was used to separate the different phases within a composite plate, i.e., matrix and carbon fibers from the porosity present in the sample, which was unachievable with conventional X-ray imaging [8, 9]. The use of XPCi allowed for the reconstruction of the different parts of the composite and for a full anisotropy analysis of the short fiber orientation. XPCi is more sensitive to effects caused by low density materials in comparison with conventional X-rays [10].

Phase-enhanced and scattering EI XPCi images for the detection of small defects were previously compared to ultrasonic C-scan imaging [11]. In this contribution, we present a comparison between EI XPCi and ultrasonic immersion C-scan imaging for the detection and classification of different types of defects present in a small carbon-based cross-ply sample suffering from severe impact damage [12]. The three types of signals retrieved from the XPCi were used to classify and identify the types of defects present in the specimen, with higher resolution than the ultrasonic immersion C-scan imaging, hence demonstrating that EI XPCi can be used for the accurate estimation of the damage extent in carbon-based composite plates.

2. MATERIALS AND METHODOLOGY

An example of this applications is presented using a 16-ply cross-ply carbon-fiber epoxy resin composite plate with severe impact damage. The lateral dimensions of the plate were measured to be 19 mm by 19 mm, and its thickness 2 mm. The sample contained an indent due to a central impact, which resulted in a small protrusion in the back of the plate, as shown in Fig. 1. The indent was measured to be approximately 4 mm in diameter, and 1.2 mm in depth. The protrusion on the back surface of the sample was measured to be approximately 5.5 mm in diameter and 0.5 mm thick.

The sample was imaged using ultrasonic immersion C-scan imaging, with a ¼ inch diameter, focused longitudinal 20 MHz transducer, as shown in Fig. 2. The transducer was placed perpendicularly at the focal length (¾ inch, 19 mm) above the sample in a water filled tank, mounted on a computer controlled scanning rig. The transducer was connected to a pulser/receiver and an amplifier. The full A-scan was recorded for each scan point using a digital storage oscilloscope and saved as a MATLAB file. The sample was positioned 3 mm above a thick steel plate to allow for double through transmission measurements. The sample was raster scanned across its entire surface with 200 μm step size. The thickness direction resolution in the sample, i.e., the calculated wavelength, was 70 μm. The measured A-scans were used to generate B-scans for comparison with EI XPCi CT slices.

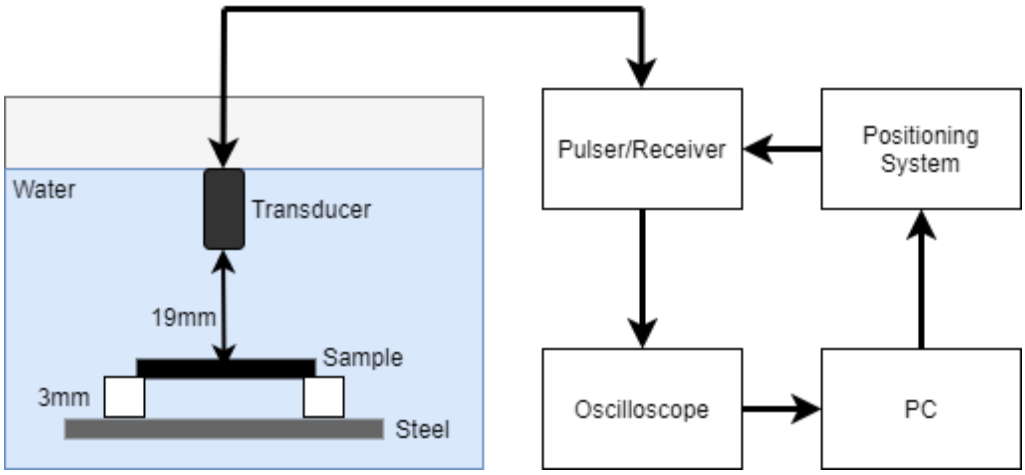

Fig. 2: Ultrasonic immersion C-scan imaging experimental setup.

EI XPCi uses a coded aperture system in order to convert the refraction angle into a variation in detected intensity, as shown in Fig. 3 (NB: not to scale; also beamlets keep diverging along the direction determined by the original cone beam). A first mask, the sample mask, is placed immediately upstream of the imaged sample, splitting the beam into an array of individual beamlets. The second mask, the detector mask, is placed in contact with the detector, thus making the regions separating adjacent pixels insensitive to incoming X-rays. When an object is placed in the beam, as shown in Fig. 3, any gradient in the unit decrement of the refractive index δ (where the entire refractive index is expressed as $n = 1 - \delta + i\beta$) will result in the deflection of the relative beamlet, and thus will lead to a change in the intensity detected by the corresponding pixel [4, 13]. This setup results in a system only sensitive to refraction changes along the x-direction. The setup for this project includes a rotating anode molybdenum X-ray source, with a 70 μm focal spot, used at 40 kVp and 20 mA current. The masks used were made of gold on a graphite substrate. The sample mask, which had apertures of 12 μm and a period of 38 μm, was placed 0.65 m away from the source, and 0.05 m upstream of the sample stage. The detector mask, with apertures of 20 μm and a period of 48 μm, was placed 0.85 m away from the source. The detector was an indirect detection flat panel CMOS detector with 50 by 50 μm^2 pixel size and a 160 μm thick CsI scintillator. However, due to light spread in the scintillator, the effective resolution of the detector was approximately 100 μm.

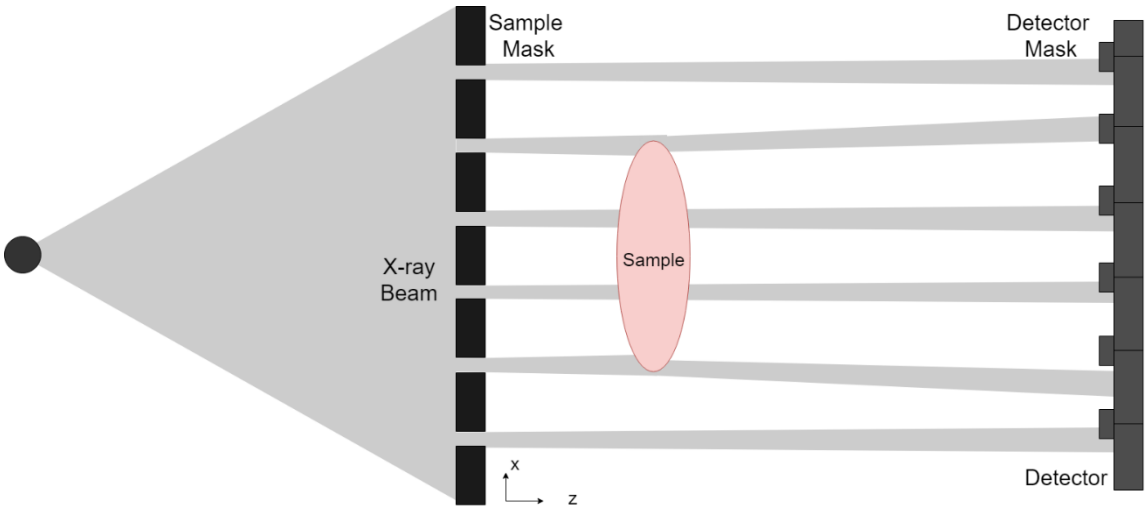

Fig. 3: EI XPCi experimental setup.

The image acquisition process included the acquisition of an illumination curve, which corresponds to the variation of the detected intensity as a function of the sample mask position with respect to the detector mask [4, 14]. In order to increase the resolution, the sample was also dithered, i.e., repositioned at different sub-pixel locations, for each sample mask position. The dithered images were then recombined in order to achieve an increased resolution. Both planar and CT images were acquired using the same experimental setup, with 1.2 s exposure time per frame. For the planar images, individual frames were acquired at 19 points on the illumination curve, plus the sample was dithered 10 times which corresponds to a tenfold increase in the overall number of frames. For the CT images, for each sample mask position, frames were acquired at 1800 projections over 360°, for a 0.2° rotation per projection. Overall, 5 points on the illumination curve were taken, with no dithering steps. A phase retrieval procedure was applied to both the planar and CT image sequences to obtain the absorption, refraction, and scattering images.

The used phase retrieval method, discussed in [13], assumes that the illumination curve can be represented by a Gaussian. The changes induced to the illumination curve by the introduction of the sample can be described as variations in the key parameters of a Gaussian: its amplitude is decreased by absorption, its center position is shifted due to refraction, and its broadening is caused by ultra-small angle scattering. The phase retrieval algorithm fits a Gaussian to the illumination curve before and after the introduction of the sample, and compares the Gaussians from the sample images to the baseline images to extract the above three parameters. Following the basic algorithm described in [13], the retrieval method was upgraded to account for the crosstalk between the pixels in the detector [15]. The new resulting algorithm fits three overlapping Gaussian distributions, separated by the sample mask period, to three adjacent pixels. The coefficients of the central Gaussian, which corresponds to the central pixel, is then used for the retrieval of phase, attenuation, and scattering.

3. RESULTS AND DISCUSSION

Planar images of the sample were taken, and the absorption, refraction and scattering images were retrieved, as shown in Fig. 4. The impact has a round outline in the absorption images, with the intensity variation across the damaged area indicating a variation in the thickness of the sample, due to material displacement caused by the impact damage.

However, the refraction, and especially the scattering image shows a square outline shape of the damage. The refraction images highlight the interface of features within the damaged area, mostly cracks and edges of the delamination (verified from the CT images [12]), visible as a long dark stripe on the left-hand side of the refraction image in Fig. 4 (arrow). The 1D sensitivity of the system is apparent in the refraction image. Samples need to be rotated and scanned again in order to obtain 2D sensitivity. The scattering images show sub-pixel features, and the shape of the signal observed in the planar images represents the degree of micro-damage in the plate. Defects such as fiber damage and micro-matrix cracks accompanying the damage in the sample are assumed to be the main cause for the scattering signal, as the damage appears more square in shape thus following the cross-ply arrangement of the fibers.

Retrieved CT images were reconstructed and overlaid as RGB images, as shown in Fig. 5 and 6, with absorption represented in blue, refraction in green and scattering in red. The CT slices are compared with the corresponding ultrasonic B-scans showing the same transversal cut through the sample. The damage in the sample is clearly visible, spreading radially from the point of impact and through the thickness of the sample, both in the CT and ultrasonic B-scan images.

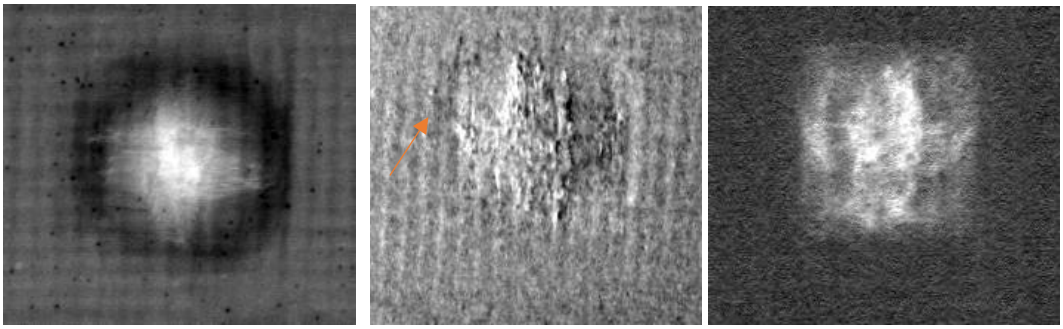

Fig. 4: Planar EI XPCi absorption (left), refraction (center) and scattering (right) images.

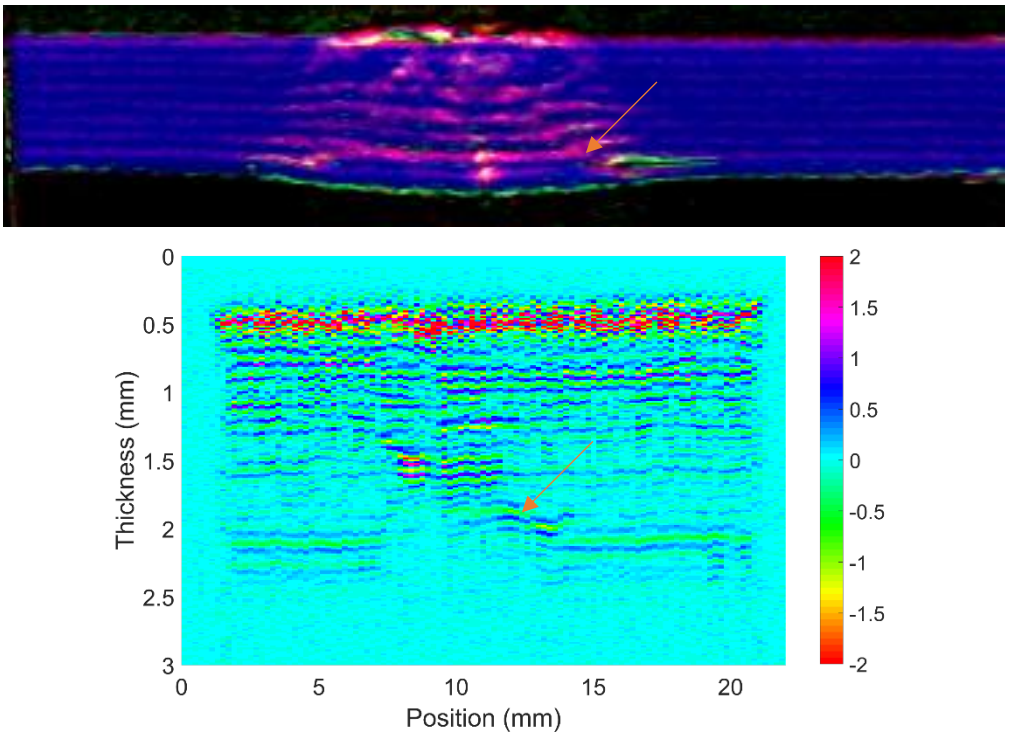

Fig. 5: CT slice showing edge of delamination (top), compared with corresponding B-scan from ultrasonic imaging (bottom).

The refraction signal, shown in green, clearly highlights interfaces inside the sample, as well as the protrusion at the back of the sample. The edge of a delamination, represented by an arrow in the CT slice on Fig. 5, is also seen (and highlighted by an arrow) in the ultrasonic image. This delamination was later observed to be doughnut-shaped, around the central impact. The presence of the delamination is only visible in the refraction signal, thanks to its ability to highlight interfaces within in the sample. On a quantitative level, the delamination was determined to be located about 0.3 mm above the back surface on both the X-ray and ultrasonic images, and was approximately 5 mm at its longest in both signals. A strong scattering signal can also be observed around the delamination, as well as across the damaged area caused by the indent, which indicates the presence of sub-pixel features accompanying the delamination and across the plies throughout the damaged area. Their sub-pixel nature makes these features not resolvable, but they could indicate that the delamination extends further than indicated by the refraction signal. The strong scattering signal can also indicate the presence of further micro-damage around the delamination and across the damaged area of the sample, such as displaced fibers and matrix or micro-cracks due the impact.

This effect is more clearly visible in Fig. 6, which shows a slice taken closer to the center of the impact in the sample, accompanied by the corresponding ultrasonic B-scan slice. It can be seen that no reflections can be observed in the ultrasonic image past the surface of the indent, which is an indication of strong damage. The lack of information past the defect closest to the surface is a big disadvantage of ultrasonic imaging, which can be addressed by using X-ray imaging. In fact, it can be seen from the X-ray slice that a crack was formed across the thickness of the sample, and strong damage (seen as yellow on the slice, resulting from a combination of strong refraction and scattering signals) is observed across the indent. Here too, a strong scattering signal can be observed across the ply layers throughout the damaged area, indicating that the large defects extend further than indicated by the system resolution (as scattering results from sub-pixel features), or that some further micro-defects are accompanying the main damage, or both.

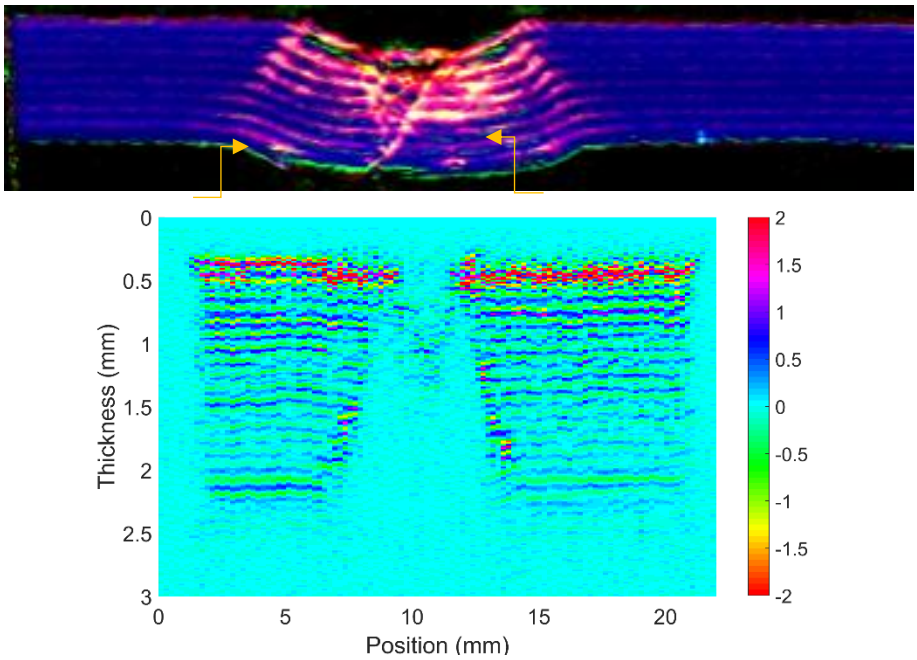

Fig. 6: CT slice showing indent and crack through thickness of sample (top), compared with corresponding B-scan from ultrasonic imaging (bottom).

Small refraction signals can be observed between the scattering signals at the ply interfaces, indicated by arrows in Fig. 6, showing small delaminations taking place at the ply interfaces due to the material displacement around the impact point. This type of observations is only achievable using this multi-modal imaging, where the refraction and scattering signal complement the conventional absorption images. Different signals show different types of defects present in the sample, leading to a better understanding of the types of defects involved and the extent of the damage in the sample. The identification of the defects in the scattering signal is not possible, however the indication of their presence provides significant additional information on the damage extent in the sample. The type of signal in which the defects manifest gives a better indication of the type and scale of damage involved, and thus allows a better estimation of the types of damage as well as their extent and distribution across the damaged area, which was unachievable so far using ultrasonic imaging or conventional radiography.

4. CONCLUSIONS

EI XPCi is an X-ray imaging technique allowing for the simultaneous acquisition and retrieval of absorption, refraction and scattering images. It was used to investigate damage in a small composite specimen with severe impact damage. EI XPCi allowed to observe and estimate the nature of defects within the sample, with the refraction and scattering images complementing the conventional absorption images. These complementary signals allowed for a better identification of the defects involved, and thus for a better understanding of the damage extent in the sample. The scattering signal, which shows sub-pixel features, provided information regarding the micro-damage accompanying the main defects. The refraction signal in the CT images allowed for the detection of multiple delaminations across the sample thickness, as well as a crack going across the sample thickness at the impact. These features were not observed in the planar EI XPCi images, nor the ultrasonic B-scan images. It can thus be concluded that EI XPCi imaging, especially when combined with CT scanning, can provide a more precise tool for damage detection and localization, as well as for quantitative evaluation of damage in composite plates.

REFERENCES

[1] Richardson, M. and Wisheart, M., "Review of Low-velocity Impact Properties of Composite Materials," Compos. Part A **27**, 1123–1131 (1996).

[2] Scott, I.G. and Scala, C.M., "A Review of Non-Destructive Testing of Composite Materials," NDT Int. **15**, 75–86 (1982).

[3] Agyei, R.F. and Sangid, M.D., "A Supervised Iterative Approach to 3D Microstructure Reconstruction from Acquired Tomographic Data of Heterogeneous Fibrous Systems," Compos. Struct. **206**, 234–246 (2018).

[4] Olivo, A. and Castelli, E., "X-ray phase contrast imaging: From synchrotrons to conventional sources," Riv. del Nuovo Cim. **37**, 467–508 (2014).

[5] Endrizzi, M., Diemoz, P.C., Millard, T.P., Louise Jones, J., Speller, R.D., Robinson, I.K. and Olivo, A., "Hard X-ray dark-field imaging with incoherent sample illumination," Appl. Phys. Lett. **104**, 024106 (2014).

[6] Endrizzi, M., Vittoria, F.A., Rigon, L., Dreossi, D., Iacoviello, F., Shearing, P.R. and Olivo, A., "X-ray phase-contrast radiography and tomography with a multiaperture analyze." Phys. Rev. Lett. **118**, 243902 (2017).

[7] Cloetens, P., Pateyron-Salomé, M., Buffiere, J.Y., Peix, G., Baruchel, J., Peyrin, F. and Schlenker, M., "Observation of microstructure and damage in materials by phase sensitive radiography and tomography," J. Appl. Phys. **81**, 5878–5886 (1997).

[8] Coindreau, O., Vignoles, G. and Goyheneche, J.-M., "Multiscale X-Ray CMT of C/C composite preforms: A Tool for Properties Assessment," in Ceramic Transactions, Advances in Ceramic Matrix Composites **11**, 37–45 (2012).

[9] Cosmi, F., Bernasconi, A. and Sodini, N., "Phase contrast micro-tomography and morphological analysis of a short carbon fibre reinforced polyamide," Compos. Sci. Technol. **71**, 23–30 (2011).

[10] Mayo, S.C., Stevenson, A.W. and Wilkins, S.W., "In-Line Phase-Contrast X-ray Imaging and Tomography for Materials Science," Materials **5**, 937–965 (2012).

[11] Endrizzi, M., Murat, B.I.S., Fromme, P. and Olivo, A., "Edge-illumination X-ray dark-field imaging for visualising defects in composite structures," Compos. Struct. **134**, 895-899 (2015).

[12] Shoukroun, D., Massimi, L., Iacoviello, F., Endrizzi, M., Bate, D., Olivo, A. and Fromme, P., "Enhanced composite plate impact damage detection and characterisation using X-Ray refraction and scattering contrast combined with ultrasonic imaging," Compos. Part B **181**, 107579 (2020).

[13] Olivo, A. and Speller, R., "Modelling of a novel x-ray phase contrast imaging technique based on coded apertures," Phys. Med. Biol. **52**, 6555–6573 (2007).

[14] Endrizzi, M., "X-ray phase-contrast imaging," Nucl. Inst. Methods Phys. Res. A **830**, 407 (2017).

[15] Maughan Jones, C.J., Vittoria, F.A., Olivo, A., Endrizzi, M. and Munro, P.R.T, "Retrieval of weak x-ray scattering using edge illumination," Opt. Lett. **43**, 3874 (2018).